AAC Journals.ASM.org

TXA709, an FtsZ-Targeting Benzamide Prodrug with Improved Pharmacokinetics and Enhanced *In Vivo* Efficacy against Methicillin-Resistant *Staphylococcus aureus*

Malvika Kaul,[a] Lilly Mark,[b,c] Yongzheng Zhang,[b] Ajit K. Parhi,[b,c] Yi Lisa Lyu,[a] Joan Pawlak,[d] Stephanie Saravolatz,[d] Louis D. Saravolatz,[d,e] Melvin P. Weinstein,[f,g] Edmond J. LaVoie,[c] Daniel S. Pilch[a]

Department of Pharmacology, Rutgers Robert Wood Johnson Medical School, Piscataway, New Jersey, USA[a]; TAXIS Pharmaceuticals, Inc., North Brunswick, New Jersey, USA[b]; Department of Medicinal Chemistry, Ernest Mario School of Pharmacy, Rutgers-The State University of New Jersey, Piscataway, New Jersey, USA[c]; St. John Hospital and Medical Center, Detroit, Michigan, USA[d]; Wayne State University School of Medicine, Detroit, Michigan, USA[e]; Departments of Medicine (Infectious Disease)[f] and Pathology and Laboratory Medicine[g], Rutgers Robert Wood Johnson Medical School, New Brunswick, New Jersey, USA

The clinical development of FtsZ-targeting benzamide compounds like PC190723 has been limited by poor drug-like and pharmacokinetic properties. Development of prodrugs of PC190723 (e.g., TXY541) resulted in enhanced pharmaceutical properties, which, in turn, led to improved intravenous efficacy as well as the first demonstration of oral efficacy *in vivo* against both methicillin-sensitive *Staphylococcus aureus* (MSSA) and methicillin-resistant *S. aureus* (MRSA). Despite being efficacious *in vivo*, TXY541 still suffered from suboptimal pharmacokinetics and the requirement of high efficacious doses. We describe here the design of a new prodrug (TXA709) in which the Cl group on the pyridyl ring has been replaced with a CF_3 functionality that is resistant to metabolic attack. As a result of this enhanced metabolic stability, the product of the TXA709 prodrug (TXA707) is associated with improved pharmacokinetic properties (a 6.5-fold-longer half-life and a 3-fold-greater oral bioavailability) and superior *in vivo* antistaphylococcal efficacy relative to PC190723. We validate FtsZ as the antibacterial target of TXA707 and demonstrate that the compound retains potent bactericidal activity against *S. aureus* strains resistant to the current standard-of-care drugs vancomycin, daptomycin, and linezolid. These collective properties, coupled with minimal observed toxicity to mammalian cells, establish the prodrug TXA709 as an antistaphylococcal agent worthy of clinical development.

Bacterial resistance has emerged as a global problem. The Centers for Disease Control and Prevention (CDC) have identified methicillin-resistant *Staphylococcus aureus* (MRSA) and vancomycin-resistant *S. aureus* (VRSA) as being two major antibiotic resistance threats (1). Typically, MRSA strains are resistant not only to the penicillins but also to other classes of antibiotics, including the tetracyclines, the macrolides, the aminoglycosides, and clindamycin (2–4). Current standard-of-care (SOC) drugs for the treatment of MRSA infections are therefore limited to a few drugs, which include vancomycin, daptomycin, and linezolid (3). However, resistance to these SOC drugs is already on the rise, and the clinical utility of these drugs is likely to diminish in the future (3, 5–9).

The bacterial protein FtsZ has been identified as an appealing new target for the development of antibiotics that can be used to treat infections caused by multidrug-resistant (MDR) bacterial pathogens (10–14). The appeal of FtsZ as an antibiotic target lies in the essential role that the protein plays in bacterial cell division (cytokinesis). Furthermore, FtsZ is prokaryote specific with no known eukaryotic homolog. FtsZ self-polymerizes in a GTP-dependent manner to form a ring-like structure (the Z-ring) at midcell that serves as a scaffold for the recruitment and organization of other critical components for proteoglycan synthesis, septum formation, and cell division (15–20).

The substituted benzamide derivative PC190723 has been shown to inhibit bacterial cell division through disruption of FtsZ function (21–24). PC190723 is associated with potent bactericidal activity against *Staphylococcus* spp., including MRSA (23, 24). However, the clinical development of this compound has been hindered by poor pharmaceutical and pharmacokinetic properties. We have previously reported the design and characterization of two prodrugs of PC190723 (TXY436 and TXY541) with physicochemical properties that significantly enhance the ease of formulation in vehicles suitable for *in vivo* administration (25, 26). While TXY436 and TXY541 were both orally and intravenously efficacious *in vivo* against MRSA, the doses required for efficacy were high, and their pharmacokinetic properties were suboptimal (25, 26). Here we describe a new prodrug (TXA709) of an FtsZ-targeting benzamide compound (TXA707) with enhanced metabolic stability, improved pharmacokinetic properties, and superior *in vivo* efficacy versus MRSA. We provide results that highlight TXA709 as an attractive lead agent for clinical development.

Received 24 March 2015 **Returned for modification** 15 April 2015
Accepted 27 May 2015

Accepted manuscript posted online 1 June 2015

Citation Kaul M, Mark L, Zhang Y, Parhi AK, Lyu YL, Pawlak J, Saravolatz S, Saravolatz LD, Weinstein MP, LaVoie EJ, Pilch DS. 2015. TXA709, an FtsZ-targeting benzamide prodrug with improved pharmacokinetics and enhanced *in vivo* efficacy against methicillin-resistant *Staphylococcus aureus*. Antimicrob Agents Chemother 59:4845–4855. doi:10.1128/AAC.00708-15.

Address correspondence to Daniel S. Pilch, pilchds@rwjms.rutgers.edu.

Supplemental material for this article may be found at http://dx.doi.org/10.1128/AAC.00708-15.

doi:10.1128/AAC.00708-15

MATERIALS AND METHODS

Bacterial strains. Methicillin-resistant *S. aureus* clinical strains ($n = 30$) were isolated from patients admitted to St. John Hospital and Medical Center (SJHMC) ($n = 20$) in Detroit, MI, or to Robert Wood Johnson University Hospital (RWJUH) ($n = 10$) in New Brunswick, NJ. The MRSA isolates were cultured from blood ($n = 26$), wound tissue ($n = 2$), pleural fluid ($n = 1$), and arm drainage ($n = 1$). Daptomycin-nonsusceptible *S. aureus* (DNSSA) isolates ($n = 7$) were cultured from blood samples collected from patients at SJHMC. Vancomycin-intermediate *S. aureus* (VISA) isolates ($n = 20$) were obtained from 20 patients. The VISA isolates were cultured from blood ($n = 12$), wound tissue ($n = 1$), bile ($n = 1$), cerebral spinal fluid ($n = 1$), and an unknown source ($n = 5$). Vancomycin-resistant *S. aureus* (VRSA) isolates ($n = 11$) were obtained from 11 patients, with these isolates being cultured from wound tissue ($n = 8$), prosthetic knee drainage ($n = 1$), urine ($n = 1$), and a catheter exterior ($n = 1$). Linezolid-nonsusceptible *S. aureus* (LNSSA) isolates ($n = 6$) were cultured from blood ($n = 2$), sputum ($n = 1$), and an unknown source ($n = 3$). The VRSA, 17 of the VISA, and 4 of the LNSSA isolates were provided by the Network on Antimicrobial Resistance in *Staphylococcus aureus* (NARSA) for distribution by BEI Resources, NIAID, NIH. The NARSA website (http://www.narsa.net) describes the location of origin of each isolate. The remaining three VISA isolates were collected at SJHMC, and the remaining two LNSSA isolates were collected at Robinson Memorial Hospital in Ravenna, OH. Methicillin-sensitive *S. aureus* (MSSA) isolates ($n = 10$) were cultured from the blood of 10 patients at RWJUH. MRSA Mu3 was a gift from George M. Eliopoulos (Beth Israel Deaconess Medical Center, Boston, MA), and MSSA 8325-4 was a gift from Glenn W. Kaatz (John D. Dingell VA Medical Center, Detroit, MI). All other MSSA and MRSA strains were obtained from the American Type Culture Collection (ATCC). *Bacillus subtilis* FG347 was a gift from Richard Losick (Harvard University, Boston, MA).

Compound synthesis. TXY541 and PC190723 were synthesized as described previously (25, 27). TXA707 and TXA709 were synthesized as detailed in the supplemental material.

Compound stability studies. The conversion of TXA709 to TXA707 in either cation-adjusted Mueller-Hinton (CAMH) broth (Becton, Dickinson and Co., Franklin Lakes, NJ) or 100% filtered mouse serum (Lampire Biological Laboratories, Inc., Ottsville, PA) at 37°C was monitored as described previously for the conversion of TXY541 to PC190723 (25). The mouse serum was filtered through a 0.2-μm filter before use.

***In vitro* susceptibility assays.** *In vitro* susceptibility assays were conducted with TXA707, TXA709, and PC190723 using vancomycin-HCl, daptomycin, and linezolid as comparator control antibiotics (all obtained from Sigma). Determinations of MICs and minimal bactericidal concentrations (MBCs) were conducted in duplicate according to Clinical and Laboratory Standards Institute (CLSI) guidelines (28). Microdilution assays with CAMH broth were used to determine the MICs of all agents. For the daptomycin assays, calcium was added to a final concentration of 50 mg/liter. The MIC is defined as the lowest compound or drug concentration at which there is no visible growth after 16 to 24 h of incubation. MBC is defined as the compound or drug concentration that reduced the number of viable cells by ≥99.9%, as determined by colony counts.

Assay for metabolism of TXY541 and TXA709 in the presence of mouse and human hepatocytes. Metabolism experiments were conducted by SAI Life Sciences Ltd. (Pune, India). Mouse hepatocytes, human hepatocytes, and cryopreserved hepatocyte recovery medium (CHRM) were obtained from Invitrogen BioServices India Pvt. Ltd. Cryopreserved hepatocytes were revived in CHRM supplemented with Krebs-Henseleit buffer (KHB), pH 7.4 (Sigma). A 500-μl cell suspension containing 2×10^6 cells/ml was added to individual wells of 24-well plates and incubated at 37°C for 15 min. Duplicate reactions were initiated by adding 500 μl of test compound diluted in KHB (prewarmed at 37°C) and further incubated at 37°C for 0 and 60 min with gentle shaking. The final cell density was 1×10^6 cells/ml, and the final concentration of the test compound was 10 μM. Reactions were terminated by adding 1 ml of ice-cold acetonitrile to a final volume of 2 ml. The terminated reaction mixtures from each well were transferred to individual tubes and sonicated for 5 min prior to centrifugation at 2,147 × *g* for 15 min at 4°C. A 1.2-ml aliquot of each supernatant was then transferred to a clean tube, and the metabolites were identified by liquid chromatography/tandem mass spectrometry (LC/MS-MS) analysis. Testosterone (Sigma) and 7-OH-coumarin (Apin Chemicals Ltd.) were used as positive controls.

Pharmacokinetic studies. Pharmacokinetic experiments in male BALB/c mice were conducted by SAI Life Sciences Ltd. as described previously (25). When used, 1-aminobenzotriazole (ABT) was administered orally at a standard dose of 50 mg/kg of body weight (29) 1 h prior to administration of the test prodrug (TXY541 or TXA709) formulated in 10 mM citrate, pH 2.6. Concentrations of the prodrug products PC190723 and TXA707 in plasma were quantified by LC/MS-MS, with the lower limits of quantitation (LLOQ) being 10.02 and 4.93 ng/ml, respectively.

Plasma protein binding studies. Plasma protein binding studies of TXA707 were conducted by SAI Life Sciences Ltd. using human, dog, rat, and mouse plasma. Protein binding was measured via rapid equilibrium dialysis (RED) using an RED device (Thermo Scientific) containing dialysis membrane with a molecular mass cutoff of 8,000 Da. Each plasma type was spiked in triplicate with 5 μM TXA709. Dialysis was then performed with shaking (at 100 rpm) for 4 h at 37°C, as per the manufacturer's recommendation. Following dialysis, the concentration of TXA707 in each well (both plasma and buffer side) was quantified by LC/MS-MS, and the resulting peak area ratios were used to determine the percentages of compound unbound and bound to plasma proteins.

***S. aureus* FtsZ polymerization assay.** *S. aureus* FtsZ was expressed and purified as described previously (30). Polymerization of *S. aureus* FtsZ was monitored as described previously (26), with the exception that FtsZ was used at a concentration of 15 μM.

Fluorescence microscopy. Fluorescence microscopy studies with *B. subtilis* FG347 were conducted as described previously (26), with the exception that the bacteria were cultured for 2 h in the presence of dimethyl sulfoxide (DMSO) vehicle or 4 μg/ml TXA707 (8× MIC).

Transmission electron microscopy. Log-phase MSSA 8325-4 cells were cultured in CAMH broth at 37°C for 0, 1, 4, or 9 h in the presence of DMSO (solvent vehicle) or TXA707 at a concentration of 4 μg/ml (8× MIC). At each time point, a 1-ml sample was withdrawn from the culture and centrifuged at 16,000 × *g* for 3 min at room temperature. The supernatant was removed, and the bacterial pellet was washed with 1 ml of phosphate-buffered saline (PBS). The final bacterial pellet was fixed by resuspension in 500 μl of 0.1 M cacodylate buffer (pH 7.2) containing 2.5% glutaraldehyde and 4% paraformaldehyde. The fixed bacterial cells were then postfixed in buffered osmium tetroxide (1%), subsequently dehydrated in a graded series of ethanol, and embedded in epon resin. Thin sections (90 nm) were cut on a Leica EM UC6 ultramicrotome. Sectioned grids were then stained with a saturated solution of uranyl acetate and lead citrate. Images were captured with an AMT XR111 digital camera at 80 kV on a Philips CM12 transmission electron microscope.

Assay for FOR and identification of resistant *ftsZ* mutations. Frequency of resistance (FOR) studies were conducted as described elsewhere (25), and the *ftsZ* genes in resistant mutants were sequenced (30).

***In vivo* efficacy assays.** Antistaphylococcal efficacy *in vivo* was assessed in a mouse peritonitis model of systemic infection, as well as in a mouse tissue (thigh) model of infection. The experimental details associated with the *in vivo* efficacy studies are described in the supplemental material.

MTT cytotoxicity assay. The cytotoxicity of TXA709 was assessed in human cervical cancer (HeLa) and Madin-Darby canine kidney (MDCK) epithelial cells using a 4-day continuous 3-(4,5-dimethylthiazol-2-yl)-2,5-diphenyltetrazolium bromide (MTT) assay as described previously (31), with vehicle and the anticancer drug camptothecin serving as negative and positive controls, respectively. TXA707 was not included in these characterizations, due to its limited solubility at the higher concentrations necessitated by the assay.

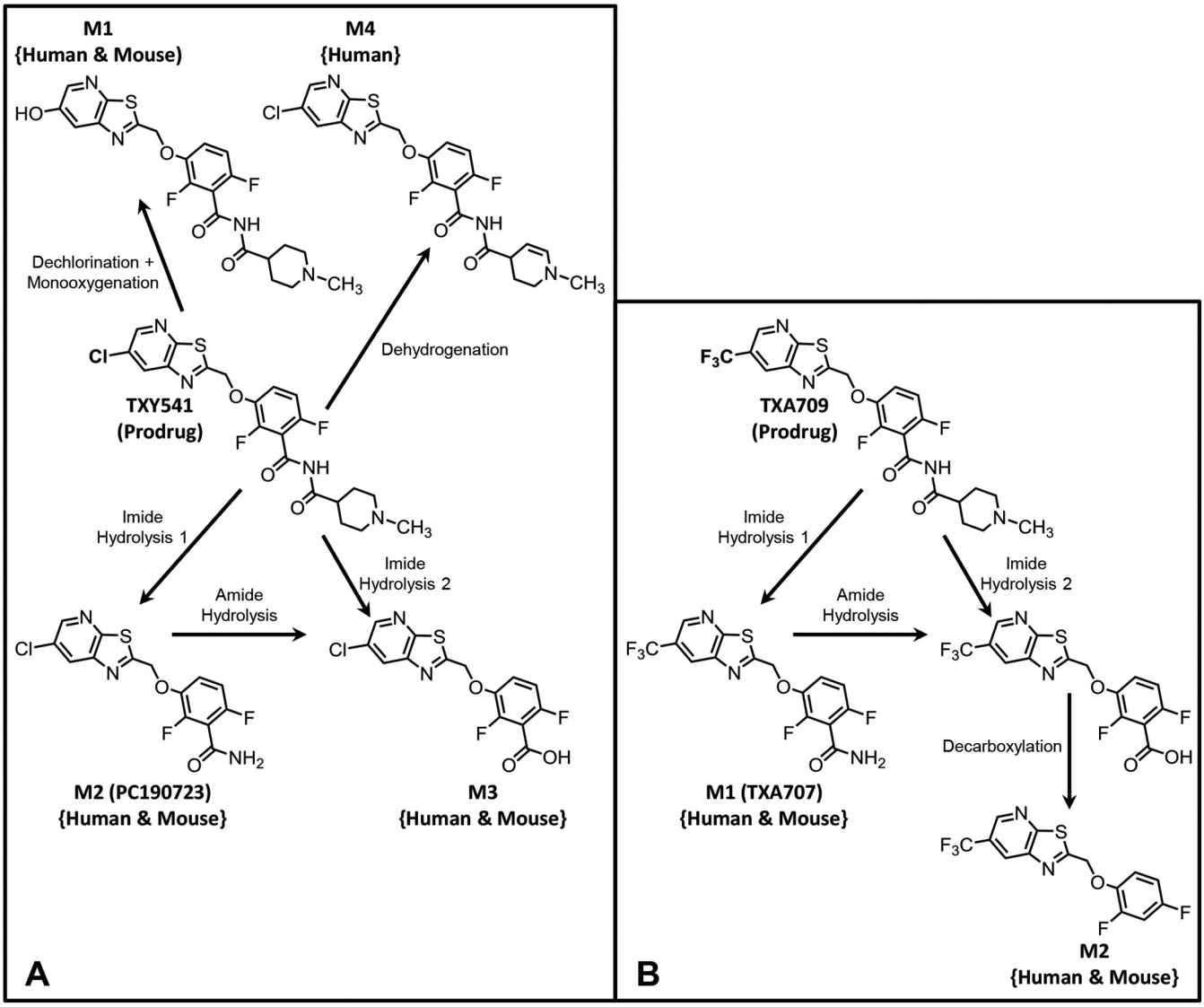

FIG 1 Metabolites of the prodrugs TXY541 (A) and TXA709 (B) that are observed upon exposure to either human or mouse hepatocytes for 60 min at 37°C.

RESULTS AND DISCUSSION

Metabolic attack of the Cl atom on the pyridyl ring of the narrow-spectrum prodrug TXY541 results in suboptimal pharmacokinetics of the active product PC190723. In our previous studies, we demonstrated that the oral and intravenous doses of the prodrug TXY541 required for efficacy in mouse models of MRSA and MSSA infection are high (96 to 192 mg/kg) due to the rapid elimination and modest oral bioavailability of the active product PC190723 (25). As a first step toward understanding the basis for the rapid elimination of PC190723 upon TXY541 administration, we conducted a metabolic study of TXY541 in the presence of either mouse or human hepatocytes. Several metabolites were observed in the presence of both mouse and human hepatocytes (Fig. 1A). The active product PC190723 was one of these metabolites (M2), detected by mass spectrometry peak analysis at an abundance of ~20% with mouse and ~30% with human hepatocytes. An even more abundant metabolite (M1; detected at an abundance of ~70% with mouse and ~50% with human hepatocytes) was one resulting from the dechlorination and subsequent monooxygenation of TXY541. Thus, the Cl atom on the pyridyl ring of TXY541 appears to be susceptible to metabolic dehalogenation.

Dehalogenation and oxygenation reactions are typically catalyzed by phase I cytochrome P450 (CYP) enzymes. We therefore hypothesized that pretreatment with a CYP inhibitor would retard the elimination of PC190723. To this end, we assessed the impact of pretreatment with CYP inhibitor 1-aminobenzotriazole on the pharmacokinetics of PC190723 in mice following administration of TXY541. As shown in Table 1, pretreatment with ABT resulted in an elimination half-life ($t_{1/2}$) of 1.95 h, a value approximately 3.5 times greater than that observed in the absence of ABT (0.56 h). This increased $t_{1/2}$ results from a correspondingly reduced clearance (CL) (13.2 versus 55.1 ml/min/kg). Thus, inhibition of CYP enzymatic activity with ABT retards the elimination of PC190723 upon administration of the TXY541 prodrug.

TABLE 1 Pharmacokinetic parameters of PC190723 and TXA707 following administration of their respective prodrugs (TXY541 and TXA709) to male BALB/c mice[a]

Prodrug administered	Dose (mg/kg), route of administration	ABT pretreatment	Product measured	t_{max} (h)	C_{max} (ng/ml)	AUC_{last} (h · ng/ml)	$t_{½}$ (h)	CL (ml/min/kg)	V_{ss} (liters/kg)	%F
TXY541	24, i.v.	Yes[b]	PC190723	0.50	7,491	28,589	1.95	13.20	2.11	NA
TXY541	24, i.v.	No	PC190723	0.25	6,646	7,216	0.56	55.11	2.18	NA
TXA709	24, i.v.	No	TXA707	0.50	13,794	42,299	3.65	9.40	2.02	NA
TXA709	32, p.o.	No	TXA707	1.00	9,850	53,679	2.66	NA	NA	95

[a] Parameters were calculated using the sparse sampling mode in the noncompartmental analysis (NCA) module of the Phoenix WinNonlin version 6.3 software package. ABT, 1-aminobenzotriazole; NA, not applicable; i.v., intravenous; p.o., peroral.
[b] Mice were pretreated for 1 h with 50 mg/kg ABT administered orally.

We next sought to determine whether the retarded elimination of PC190723 induced by ABT would also reduce the dose of TXY541 required for antistaphylococcal efficacy *in vivo*. In the absence of ABT, oral administration of TXY541 required a dose of 128 mg/kg for efficacy (83% survival; 5 of 6 [5/6] animals) in mice systemically infected with MSSA ATCC 19636 (Fig. 2A) and a dose of 192 mg/kg for efficacy (100% survival; 6/6) in mice systemically infected with MRSA ATCC 43300 (Fig. 2B). In contrast, with ABT pretreatment, the oral dose of TXY541 required for efficacy (100% survival; 6/6) in both MSSA- and MRSA-infected mice was 64 mg/kg. Pretreatment with the CYP inhibitor therefore reduces the dose of TXY541 required for efficacy by 2- and 3.5-fold in the MSSA-infected and MRSA-infected mice, respectively.

Design of a new prodrug (TXA709) that can circumvent the CYP-mediated dechlorination/oxygenation reactions associated with TXY541. As indicated by our studies described above, the Cl atom on TXY541 is vulnerable to CYP-mediated metabolic attack. Our goal in designing an improved prodrug was to replace the Cl functionality on the pyridyl ring with an electron-withdrawing group that would not undergo dehalogenation. In addition to being resistant to metabolism, the introduced group needed to be hydrophobic in nature, as polar functionalities at this position of the pyridyl ring tend to reduce antistaphylococcal potency (32). One of the most promising new prodrugs to emerge from our design efforts is TXA709 (Fig. 1B), in which the Cl atom present in TXY541 has been replaced with a CF_3 functionality. Just as hydrolysis of TXY541 yields the active product PC190723, corresponding hydrolysis of TXA709 yields an active product that we designate TXA707 (Fig. 1B). In fact, TXY541 and TXA709 have similar prodrug-to-product conversion kinetics. Figure 3 shows high-performance liquid chromatography (HPLC) chromatograms demonstrating the time-dependent conversion of TXA709 to TXA707 at 37°C in two different media at pH 7.4, CAMH broth (used for culturing *S. aureus*) and mouse serum. Analysis of the TXA709 peak areas yielded conversion half-lives (7.7 ± 0.1 h in CAMH broth and 3.0 ± 0.2 min in mouse serum) of magnitude similar to that of half-lives previously reported for the conversion of TXY541 to PC190723 (8.2 ± 0.4 h in CAMH broth and 3.4 ± 0.2 min in mouse serum) (25). In other words, substitution of CF_3 for Cl on the pyridyl ring does not significantly alter the prodrug-to-product conversion kinetics.

The CF_3 functionality of TXA709 is resistant to metabolic attack in the presence of mouse and human hepatocytes. To determine if the introduced CF_3 functionality of TXA709 imparts resistance to metabolism, we examined the metabolism of TXA709 in the presence of mouse or human hepatocytes. With both hepatocyte types, only two metabolites were observed (Fig. 1B), with the major metabolite (M1) being the active product TXA707. Significantly, no metabolic reactions targeting the CF_3 group were observed, confirming the metabolic stability of this functionality.

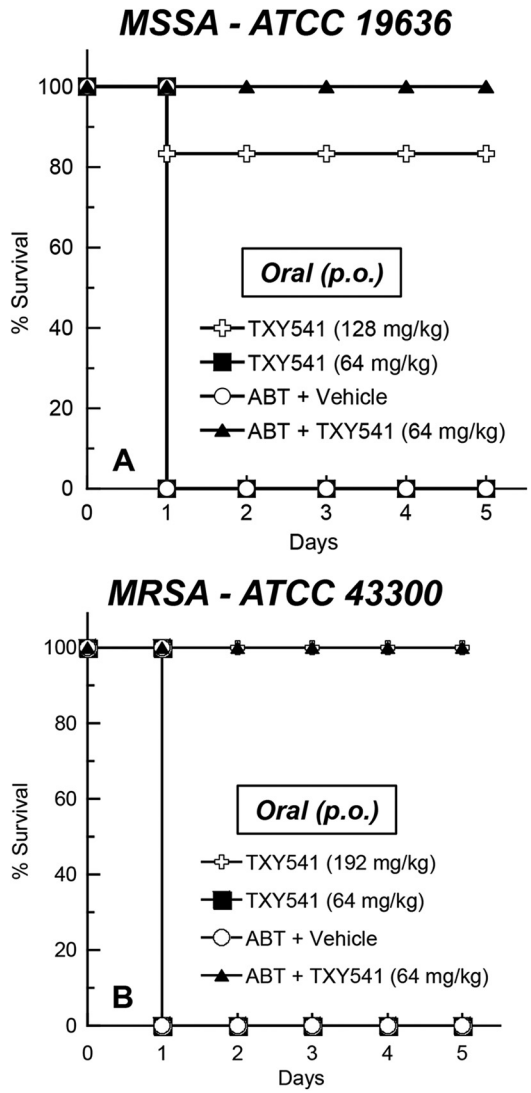

FIG 2 Impact of pretreatment with 1-aminobenzotriazole (ABT) on the oral efficacy of TXY541 in a mouse peritonitis model of systemic infection with MSSA ATCC 19636 (A) or MRSA ATCC 43300 (B). ABT was administered orally at a dose of 50 mg/kg 1 h prior to infection.

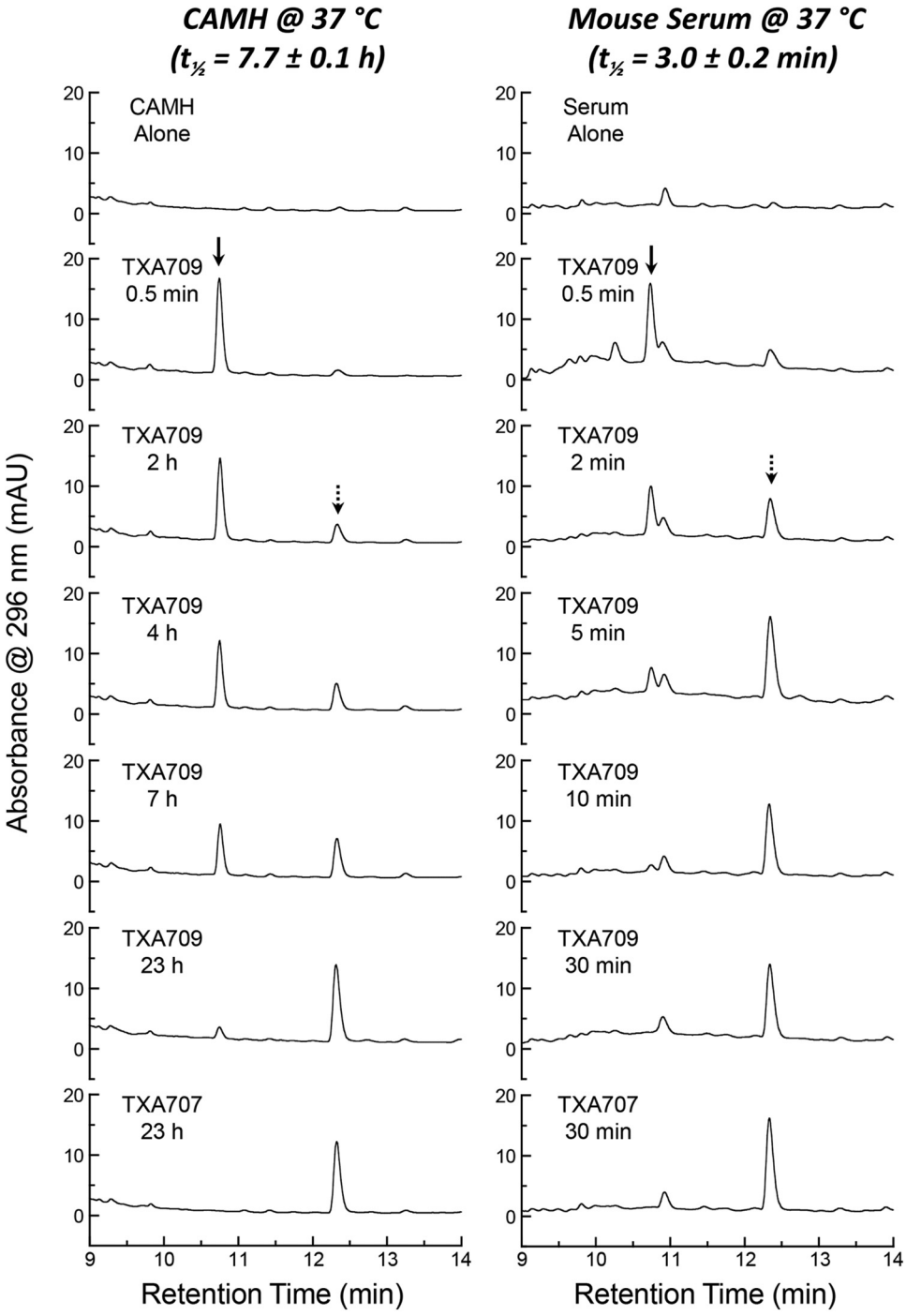

FIG 3 Reverse-phase HPLC chromatograms of 20 μM TXA709 after the indicated times of incubation at 37°C in CAMH broth (left) or mouse serum (right). For comparative purposes, the corresponding chromatograms of 20 μM TXA707 after incubation for 23 h in CAMH (bottom left) or 30 min in mouse serum (bottom right) are also presented. The baseline chromatograms of CAMH broth and mouse serum alone are shown at the tops of the left and right panels, respectively. The solid arrows indicate the peaks corresponding to TXA709, while the dashed arrows indicate the peaks corresponding to TXA707. The TXA709-to-TXA707 conversion half-life ($t_{1/2}$) in each medium is indicated.

TXA709 is associated with improved pharmacokinetic properties relative to TXY541. We next sought to determine whether the metabolic stability of TXA709 would translate to improved pharmacokinetic properties in mice. To this end, we evaluated the plasma pharmacokinetics of the TXA709 prodrug and its TXA707 product following both intravenous (i.v.) and oral (p.o.) administration of TXA709 to mice. TXA709 was not detectable in the plasma at any time point (from 0.08 to 24 h) following administration by either route. In contrast, the concentration of TXA707 in plasma was detectable and quantifiable up to 24 h following

TABLE 2 Protein binding of TXA707 in mouse, human, dog, and rat plasma[a]

Species	% protein bound
Mouse	85.9 ± 0.4
Human	90.9 ± 0.5
Dog	90.9 ± 0.3
Rat	90.8 ± 1.3

[a] Values reflect the means ± SD from three replicate experiments.

both i.v. and p.o. administration of TXA709. This observation is consistent with the rapid conversion of TXA709 to TXA707 that we observed in the presence of mouse serum at 37°C (Fig. 3).

The time-dependent concentrations of TXA707 in plasma after either p.o. or i.v. administration of TXA709 are graphically depicted in Fig. S1 in the supplemental material. Pharmacokinetic analysis of these data yielded pharmacokinetic parameters summarized in Table 1. A comparison of these parameters with the corresponding pharmacokinetic parameters for PC190723 following TXY541 administration reveals that TXA707 is associated with an elimination $t_{1/2}$ following i.v. administration of TXA709 that is approximately 6.5 times longer than the corresponding $t_{1/2}$ of PC109723 following i.v. administration of TXY541 ($t_{1/2}$ = 3.65 h for TXA707 versus 0.56 h for PC190723). The longer $t_{1/2}$ of TXA707 relative to PC190723 is due to a correspondingly reduced CL (9.40 ml/min/kg for TXA707 versus 55.11 ml/min/kg for PC190723). In addition, the bioavailability (%F) of TXA707 following p.o. administration of TXA709 was found to be 95%, approximately 3.2 times the corresponding value (%F = 29.6) that we have previously shown for PC190723 following p.o. administration of TXY541 (25).

To determine whether the observed pharmacokinetic differences between TXA707 and PC190723 might be due to differences in plasma protein binding, we assessed the protein binding properties of TXA707 in mouse, human, rat, and dog plasma. The results of these studies (summarized in Table 2) revealed that TXA707 is ~86% bound to mouse plasma proteins and ~91% bound to human, rat, and dog plasma proteins. Significantly, the percentage bound to mouse plasma proteins is nearly identical to that (85.4%) previously reported for PC190723 (32), indicating that the observed pharmacokinetic differences between the two compounds do not reflect differences in plasma protein binding properties. Our collective results therefore indicate that the metabolic stability of the CF_3 moiety present in TXA709 confers the prodrug with markedly improved pharmacokinetic properties relative to TXY541, properties that include an active product with (i) reduced CL, (ii) longer elimination $t_{1/2}$, and (iii) enhanced oral bioavailability.

TXA709 and TXA707 exhibit potent bactericidal activity against clinical isolates of MRSA, VISA, VRSA, DNSSA, LNSSA, and MSSA. We evaluated the MICs and minimal bactericidal concentrations (MBCs) of TXA709 and TXA707 against a panel of 84 clinical *S. aureus* isolates, including 30 MRSA, 20 VISA, 11 VRSA, 7 DNSSA, 6 LNSSA, and 10 MSSA isolates. The results of these determinations are summarized in Table 3. The modal MIC for TXA707 was 1 μg/ml against all six types of clinical isolates tested (MRSA, VISA, VRSA, DNSSA, LNSSA, and MSSA). We observed an identical modal MIC for PC190723 against the six types of clinical isolates. Thus, the Cl-to-CF_3 change on the pyridyl ring does not diminish antibacterial potency. Note that the modal MIC of TXA707 against the MRSA isolates is similar, if not identical, to the corresponding modal MICs of vancomycin (1 μg/ml), daptomycin (1 μg/ml), and linezolid (2 μg/ml), which were included as comparator control antibiotics representative of current standard-of-care (SOC) drugs for the treatment of MRSA infections. Significantly, TXA707 maintains a modal MIC of 1 μg/ml against *S. aureus* strains that are associated with various degrees of resistance to vancomycin (VISA and VRSA), daptomycin (DNSSA), or linezolid (LNSSA). Thus, TXA707 maintains its antistaphylococ-

TABLE 3 Activities against clinical isolates of MRSA, VISA, VRSA, DNSSA, LNSSA, and MSSA[a]

	MIC (μg/ml)		MBC (μg/ml)	
Isolate and agent	Range	Modal	Range	Modal
MRSA (n = 30)				
TXA707	0.25–1	1	1–2	1
TXA709	2–4	2	2–4	4
PC190723	0.5–1	1	0.5–1	1
VAN	0.5–1	1	0.5–1	1
DAP	0.5–2	1	0.5–1	1
LZD	2–4	2	8–>8	>8
VISA (n = 20)				
TXA707	0.5–2	1	0.5–2	1
TXA709	2–4	2	2–4	2
PC190723	0.5–1	1	0.5–2	1
VAN	4–8	4	4–8	4
DAP	1–8	1	1–16	2
LZD	0.5–2	2	2–>8	>8
VRSA (n = 11)				
TXA707	0.5–1	1	1	1
TXA709	2	2	2	2
PC190723	0.5–1	1	0.5–1	1
VAN	32–>64	>64	64–>64	>64
DAP	0.25–1	1	0.25–1	1
LZD	0.5–4	2	8–>8	>8
DNSSA (n = 7)				
TXA707	0.5–1	1	1–2	1
TXA709	2–4	2	2–4	4
PC190723	0.5–1	1	0.5–1	1
VAN	1–2	2	2	2
DAP	4	4	4–8	8
LZD	1–2	2	2–>8	>8
LNSSA (n = 6)				
TXA707	1	1	1–2	1
TXA709	2	2	2–4	2
PC190723	0.5–1	1	1	1
VAN	1–2	1	1–2	1
DAP	0.5–1	0.5	0.5–1	0.5/1[b]
LZD	16–64	16	32–>64	>64
MSSA (n = 10)				
TXA707	0.5–1	0.5/1[b]	1–2	1/2[b]
TXA709	2–4	4	4–8	8
PC190723	0.5–1	1	1–2	2
VAN	1–2	1	1–4	2
DAP	1	1	ND	ND

[a] VAN, vancomycin; DAP, daptomycin; LZD, linezolid; ND, not determined. MBCs for MRSA were determined with 20 isolates.
[b] Bimodal behavior.

TABLE 4 Activities against reference quality control and laboratory strains of MRSA and MSSA

Strain	MIC (μg/ml)			
	TXA707	TXA709	PC190723	VAN
MRSA				
ATCC 43300[a]	0.5	4	0.5	2
ATCC 33591[b]	1	4	1	2
Mu3[a]	0.5	2	0.5	2
MSSA				
ATCC 19636[a]	0.5	2	0.5	1
ATCC 29213	0.5	2	1	1
8325-4[c]	0.5	2	0.5	0.5

[a] Strain used in the *in vivo* mouse systemic (peritonitis) infection studies.
[b] Strain used in the *in vivo* mouse tissue (thigh) infection studies.
[c] Strain used in the TEM studies.

cal potency even against strains for which current SOC drugs do not. While the prodrug TXA709 also exhibits activity against all 84 *S. aureus* isolates tested, its modal MICs are 2- to 4-fold higher than those of TXA707. This discrepancy likely reflects the lack of total conversion of TXA709 to TXA707, due to the slow conversion kinetics in CAMH medium ($t_{1/2} = 7.7 \pm 0.1$ h). For all the *S. aureus* isolates examined, the modal MBCs for TXA707 and TXA709 were similar, if not identical, to the corresponding modal MICs, with the difference between the modal MBCs and MICs never being >2-fold. These results indicate that the observed antibacterial activities of the compounds against the *S. aureus* isolates tested are bactericidal in nature.

For comparative purposes, we also tested the activities of TXA707 and TXA709 against quality control and laboratory strains of both MSSA and MRSA (two quality control strains and one laboratory strain each), with the results being summarized in Table 4. As expected, the antibacterial potencies of both compounds against these MSSA and MRSA strains were similar in magnitude (MIC of 0.5 to 1 μg/ml for TXA707 and 2 to 4 μg/ml for TXA709) to those observed against the clinical isolates described above. These quality control and laboratory strains of *S. aureus* were used in the *in vivo* efficacy experiments described below.

Validation of the cell division protein FtsZ as the bactericidal target of TXA707. We next sought to establish that the bactericidal activity of TXA707, the active product of the TXA709 prodrug, reflects its ability to target FtsZ. To this end, we conducted the following four series of studies.

(i) Impact on FtsZ polymerization. We and others have shown that the antibacterial activities of FtsZ-targeting benzamides like PC190723 result from overstimulation of FtsZ polymerization dynamics and stabilization of nonfunctional FtsZ polymeric structures (21–24, 26, 33, 34). Thus, as a first step in validating FtsZ as the antibacterial target of TXA707, we assessed the impact of TXA707 on the polymerization dynamics of purified *S. aureus* FtsZ using a microtiter plate-based spectrophotometric assay in which changes in FtsZ polymerization are reflected by corresponding changes in absorbance at 340 nm (A_{340}). Figure 4A shows the time-dependent A_{340} profiles of *S. aureus* FtsZ in the absence and presence of TXA707 at concentrations ranging from 0.5 to 5 μg/ml. Note that TXA707 stimulates FtsZ polymerization in a concentration-dependent manner, a behavior similar to that previously demonstrated for PC190723 (21–24, 26, 33, 34). As expected, vancomycin, included in this assay as a non-FtsZ-targeting control antibiotic, did not impact FtsZ polymerization.

(ii) Impact on FtsZ Z-ring formation. We also evaluated the impact of TXA707 on FtsZ Z-ring formation in bacteria by using fluorescence microscopy. To this end, we used a strain of *B. subtilis* (FG347) that expresses a green fluorescent protein (GFP)-tagged Z-ring marker protein (ZapA) (35). We have previously shown that PC190723 induces a filamentous phenotype in these bacteria, as well as mislocalization of FtsZ from the septal Z-ring at midcell to multiple punctate sites throughout the cell (26, 34). As shown in Fig. 4B, our studies with TXA707 have demonstrated an identical pattern of behavior, consistent with inhibition of cell division by the compound through disruption of FtsZ function.

(iii) Impact on septum formation and cell division. As a third approach to establishing TXA707 as an inhibitor of cell division,

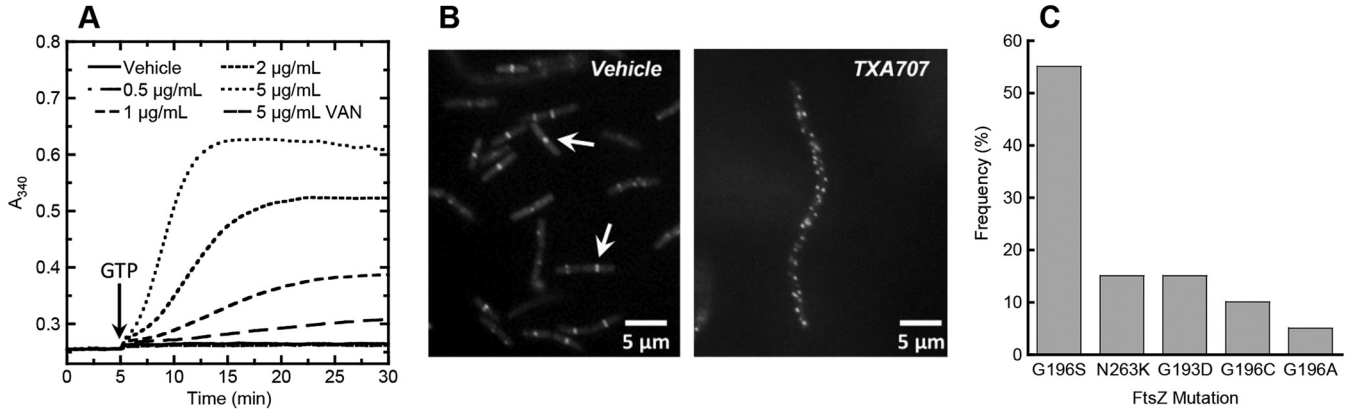

FIG 4 (A) Concentration dependence of the impact of TXA707 on the polymerization of *S. aureus* FtsZ, as determined by monitoring time-dependent changes in absorbance at 340 nm (A_{340}) at 25°C. Polymerization profiles were acquired in the presence of DMSO vehicle or the indicated concentrations of TXA707. Vancomycin (VAN) was included as a negative (non-FtsZ-targeting) control. Polymerization reactions were initiated by addition of GTP at the time indicated by the arrow. (B) Fluorescence micrographs of *B. subtilis* FG347 bacteria that express a GFP-tagged, Z-ring marker protein (ZapA). The bacteria were cultured for 2 h in the presence of DMSO vehicle (left) or 4 μg/ml TXA707 (8× MIC) (right). The arrows in the left panel highlight septal FtsZ Z-rings at midcell. (C) Relative frequency of FtsZ amino acid substitutions conferring resistance to TXA707 among 20 independently isolated TXA707-resistant clone of MRSA.

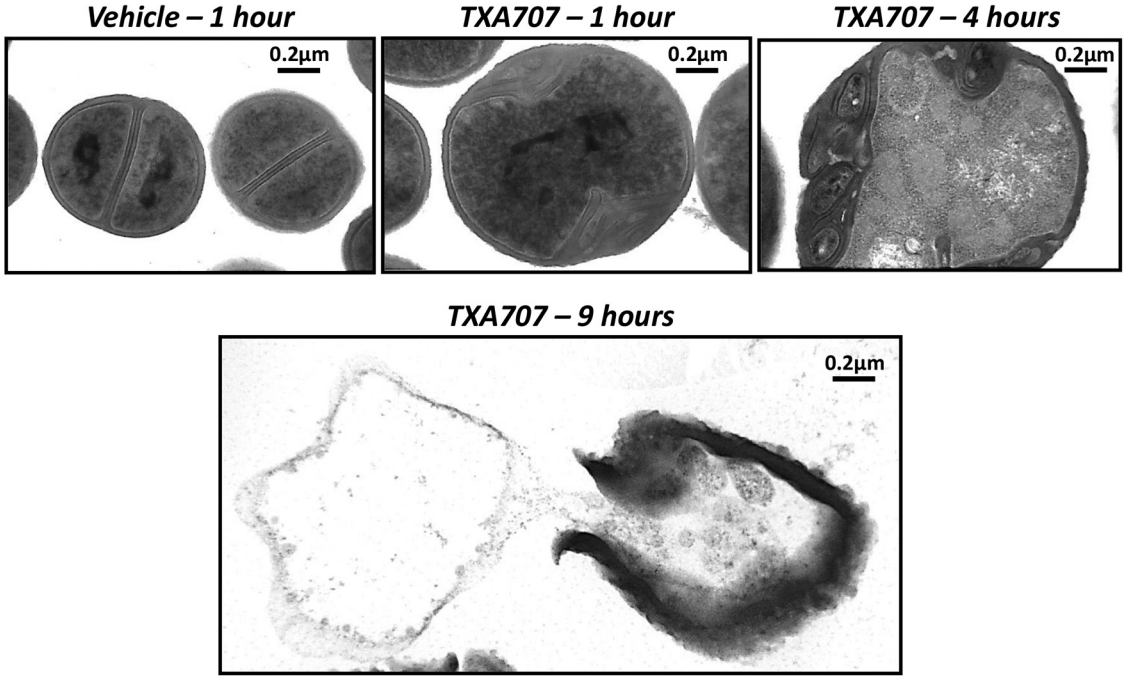

FIG 5 Transmission electron micrographs of MSSA 8325-4 bacteria treated with DMSO vehicle or 4 μg/ml TXA707 (8× MIC) for the indicated periods of time.

we also used transmission electron microscopy (TEM) to examine the impact of TXA707 on cell morphology and septum formation in MSSA 8325-4. The precise localization of FtsZ and the penicillin binding proteins (PBPs) to the septum is critical for the proper coordination of septal proteoglycan biosynthesis and cell division in *S. aureus* (18–20). The FtsZ-targeting activity of PC190723 in *S. aureus* has been shown to cause the disruption of cell division through mislocalization of both FtsZ and PBP2 (and thus septal biosynthesis) from midcell to the cell periphery (18, 20). Our TEM studies demonstrate that within 1 h of treatment with TXA707, no septa are observed in the *S. aureus* bacteria (Fig. 5). Instead, peptidoglycan synthesis appears to have shifted to discrete locations at the cell periphery. In addition, the cells become enlarged approximately 3-fold over time, eventually leading to cell lysis.

(iv) Isolation of resistance mutations that map to the FtsZ coding sequence. Perhaps the most definitive approach for validating a particular bacterial protein as the specific target of an antibacterial agent is through genetic studies demonstrating that mutations in the target protein can result in resistance. In this connection, we used a large-inoculum approach in an effort to raise spontaneous mutants of MRSA that are resistant to TXA707. This approach yielded resistant clones at a frequency of $\sim 3 \times 10^{-8}$ in MRSA ATCC 43300 and $\sim 1 \times 10^{-8}$ in an MRSA clinical isolate from a patient at RWJUH. These FOR values are similar in magnitude to those previously reported for PC190723 in various MSSA and MRSA strains (20, 23, 25). Twenty of the TXA707-resistant clones (10 from each MRSA strain) were isolated, and the *ftsZ* gene in each clone was sequenced. All 20 resistant clones carried a mutation that mapped to the *ftsZ* gene. Of the 20 clones, 11 (55%) carried a G196S mutation, 3 (15%) carried a N263K mutation, 3 (15%) carried a G193D mutation, 2 (10%) carried a G196C mutation, and 1 (5%) carried a G196A mutation (Fig. 4C). All of these FtsZ mutations have been previously shown to cause *S. aureus* resistance to PC190723 at similar relative frequencies (20, 23). Our mutational analysis is therefore fully consistent with FtsZ being the antibacterial target of TXA707.

TXA709 is associated with enhanced oral and intravenous efficacy relative to TXY541 in a mouse systemic (peritonitis) model of MSSA and MRSA infection. Armed with the *in vitro* susceptibility, FtsZ-targeting, and pharmacokinetic results described above, we next evaluated the *in vivo* antistaphylococcal efficacy of TXA709 using a mouse peritonitis model of systemic infection with *S. aureus*. In our initial studies, mice were inoculated intraperitoneally with a lethal inoculum of MSSA ATCC 19636, against which TXA707 exhibits an MIC of 0.5 μg/ml (Table 4). None of the mice treated p.o. (0/6) or i.v. (0/5) with vehicle alone survived beyond 1 day postinfection (Fig. 6A and D). In contrast, 50% (3/6) of the mice receiving a p.o. dose of 32 mg/kg TXA709 and 100% (6/6) of the mice receiving a p.o. dose of 64 mg/kg TXA709 survived the MSSA infection. Furthermore, 100% (5/5) of the mice receiving an i.v. dose of 36 or 72 mg/kg TXA709 also survived the MSSA infection. Thus, an i.v. dose of 36 mg/kg TXA709 and a p.o. dose of 64 mg/kg were sufficient for 100% survival of the MSSA infection. Significantly, these efficacious i.v. and p.o. doses of TXA709 are 2 to 2.7 times lower than the corresponding efficacious doses of TXY541 (Fig. 2).

In our next set of studies, mice were administered a lethal inoculum of MRSA ATCC 43300. None of the infected mice treated p.o. (0/6) or i.v. (0/4) with vehicle alone survived beyond 2 days postinfection (Fig. 6B and E). In striking contrast, an i.v. dose of 36 mg/kg TXA709 and a p.o. dose of 48 mg/kg TXA709 resulted in 100% survival (6/6 and 4/4 of the mice treated i.v. and p.o., respectively). Recall that the p.o. dose of TXY541 required for 100% survival in the systemic MRSA ATCC 43300 infection model was

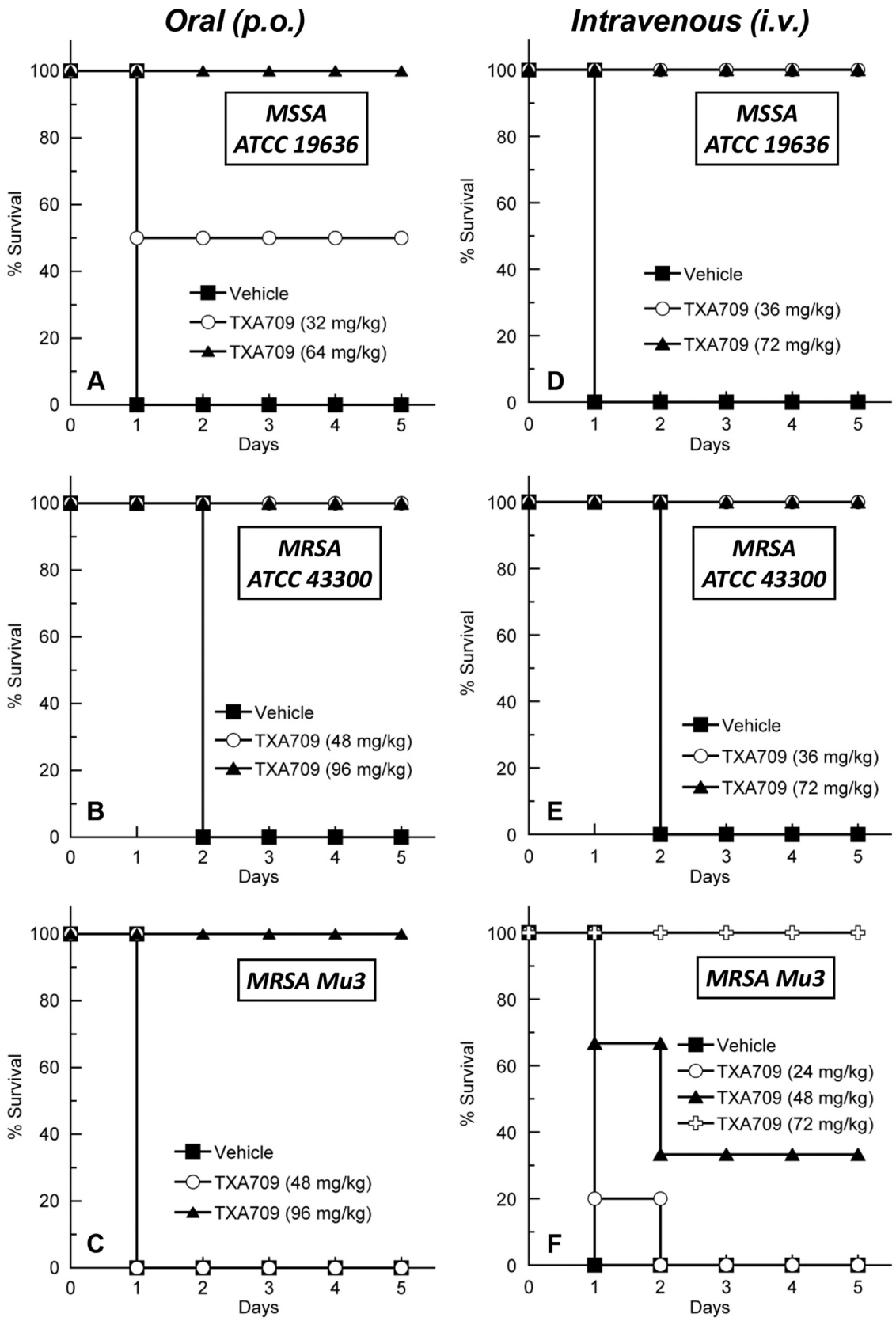

FIG 6 Oral (A to C) and intravenous (D to F) efficacy of TXA709 in a mouse peritonitis model of systemic infection with MSSA ATCC 19636 (A, D), MRSA ATCC 43300 (B, E), or MRSA Mu3 (C, F). The vehicle was 10 mM citrate (pH 2.6) in all experiments.

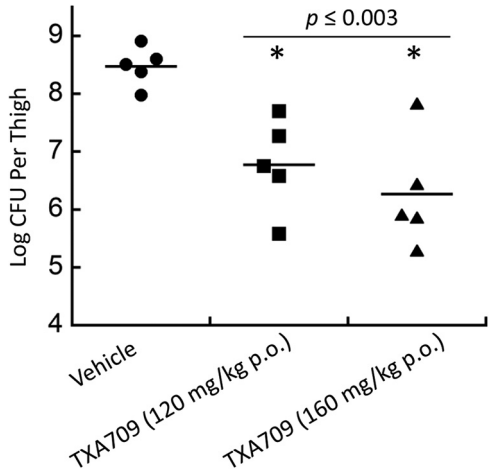

FIG 7 Oral efficacy of TXA709 in a mouse tissue (thigh) model of infection with MRSA ATCC 33591. The numbers of CFU recovered from the infected thighs after 24 h are shown. Mean CFU reductions resulting from TXA709 treatment were significant ($P \leq 0.003$).

192 mg/kg (Fig. 2), 4 times higher than the corresponding efficacious p.o. dose of TXA709 (48 mg/kg). Additional studies with mice infected with MRSA Mu3 revealed efficacious TXA709 doses of 72 mg/kg i.v. and 96 mg/kg p.o. (Fig. 6C and F). The larger doses of TXA709 required for efficacy against Mu3 relative to ATCC 43300 do not reflect a difference in the antibacterial potency of TXA707 against the two bacterial strains, as the MIC of TXA707 against either strain is 0.5 μg/ml (Table 4). Instead, the reduced efficacy of TXA709 against Mu3 compared to ATCC 43300 may reflect an enhanced virulence on the part of the Mu3 strain, the lethal inoculum for which is 2.5 times lower than that for ATCC 43300 (see the supplemental material).

In the aggregate, our *in vivo* antistaphylococcal studies demonstrate that TXA709 is associated with enhanced efficacy relative to TXY541 against systemic infections with either MSSA or MRSA.

TXA709 is also orally efficacious in a mouse tissue (thigh) model of MRSA infection. Among the pharmacokinetic properties of TXA707 upon i.v. administration of TXA709 was a volume of distribution at steady state (V_{ss}) of 2.02 liters/kg (Table 1). This V_{ss} value is approximately 3 times greater than the total water volume in the mouse (0.7 liters/kg), indicating that TXA707 distributes beyond the vascular space and into the tissue. This property is desirable for antistaphylococcal agents, since staphylococcal infections frequently occur in soft tissue. In this connection, we characterized the oral efficacy of TXA709 in a mouse tissue (thigh) model of infection with MRSA ATCC 33591. An oral dose of either 120 or 160 mg/kg TXA709 resulted in an ~2-log reduction in bacterial CFU relative to vehicle-treated mice ($P \leq 0.003$) at 24 h postinfection (Fig. 7). Previous studies with PC190723 in a mouse thigh model of MRSA infection yielded only an ~0.5-log reduction in bacterial CFU when the compound was administered orally at a dose of 200 mg/kg every 6 h over a 24-hour period (20). Viewed as a whole, these results indicate that TXA709 is orally efficacious against MRSA not only in a mouse systemic model of infection but also in a mouse tissue model of infection. Furthermore, the efficacy of orally administered TXA709 against MRSA in the mouse tissue model of infection is significantly greater than that of orally administered PC190723.

TXA709 exhibits minimal toxicity to mammalian cells. To probe for any potential mammalian cytotoxicity, we used a 4-day tetrazole (MTT)-based assay to assess the cytotoxicity of TXA709 against human cervical cancer (HeLa) and Madin-Darby canine kidney (MDCK) cells. TXA709 was found to be minimally toxic to both cell types, with 50% inhibitory concentrations (IC_{50}s) of >120 μg/ml. While these IC_{50}s reflect cell culturing conditions that include the presence of 10% fetal bovine serum, our control studies reveal a modal antistaphylococcal MIC of 2 μg/ml for TXA709 in the presence of the same percentage of serum. Thus, the large difference between the mammalian cell IC_{50}s and the antistaphylococcal MICs is due to the targeting specificity of the compound for staphylococci as opposed to serum protein binding effects.

In conclusion, TXA709 is a prodrug of a new FtsZ-targeting benzamide compound (TXA707) with enhanced metabolic stability, improved pharmacokinetic properties, and superior *in vivo* antistaphylococcal efficacy (both oral and intravenous) relative to previously identified prodrugs (TXY436 and TXY541) of PC190723. TXA707 maintains potent activity against *S. aureus* strains (e.g., MRSA, VRSA, DNSSA, and LNSSA) that are resistant to current SOC antibiotics. These characteristics, coupled with minimal cytotoxicity to mammalian cells, make the prodrug TXA709 an attractive lead compound for development into a clinically useful agent for the treatment of drug-resistant staphylococcal infections.

ACKNOWLEDGMENTS

This study was supported by research agreements between TAXIS Pharmaceuticals, Inc., and Rutgers RWJMS (D.S.P. and M.P.W.), Rutgers EMSP (E.J.L.), and SJHMC (L.D.S.).

We are indebted to Glenn W. Kaatz, Richard Losick, and George M. Eliopoulos for providing us with *S. aureus* 8325-4, *B. subtilis* FG347, and *S. aureus* Mu3, respectively. We also thank Raj Patel (Rutgers RWJMS, Core Imaging Lab) for his assistance with the TEM experiments and Giovanni Divinagracia (RWJUH) for his assistance with the *in vitro* susceptibility assays.

REFERENCES

1. **Centers for Disease Control and Prevention.** September 2013. Antibiotic resistance threats in the United States, 2013. CDC, Atlanta, GA. http://www.cdc.gov/drugresistance/threat-report-2013/.
2. **Fair RJ, Tor Y.** 2014. Antibiotics and bacterial resistance in the 21st century. Perspect Medicin Chem **6:**25–64.
3. **Moellering RC, Jr.** 2012. MRSA: the first half century. J Antimicrob Chemother **67:**4–11. http://dx.doi.org/10.1093/jac/dkr437.
4. **Otto M.** 2012. MRSA virulence and spread. Cell Microbiol **14:**1513–1521. http://dx.doi.org/10.1111/j.1462-5822.2012.01832.x.
5. **Hanaki H, Cui L, Ikeda-Dantsuji Y, Nakae T, Honda J, Yanagihara K, Takesue Y, Matsumoto T, Sunakawa K, Kaku M, Tomono K, Fukuchi K, Kusachi S, Mikamo H, Takata T, Otsuka Y, Nagura O, Fujitani S, Aoki Y, Yamaguchi Y, Tateda K, Kadota J, Kohno S, Niki Y.** 2014. Antibiotic susceptibility survey of blood-borne MRSA isolates in Japan from 2008 through 2011. J Infect Chemother **20:**527–534. http://dx.doi.org/10.1016/j.jiac.2014.06.012.
6. **Ikeda-Dantsuji Y, Hanaki H, Nakae T, Takesue Y, Tomono K, Honda J, Yanagihara K, Mikamo H, Fukuchi K, Kaku M, Kohno S, Niki Y.** 2011. Emergence of linezolid-resistant mutants in a susceptible-cell population of methicillin-resistant *Staphylococcus aureus*. Antimicrob Agents Chemother **55:**2466–2468. http://dx.doi.org/10.1128/AAC.01548-10.
7. **Mishra NN, Bayer AS, Weidenmaier C, Grau T, Wanner S, Stefani S, Cafiso V, Bertuccio T, Yeaman MR, Nast CC, Yang SJ.** 2014. Phenotypic and genotypic characterization of daptomycin-resistant methicillin-resistant *Staphylococcus aureus* strains: relative roles of *mprF* and *dlt* operons. PLoS One **9:**e107426. http://dx.doi.org/10.1371/journal.pone.0107426.

8. **Mishra NN, McKinnell J, Yeaman MR, Rubio A, Nast CC, Chen L, Kreiswirth BN, Bayer AS.** 2011. *In vitro* cross-resistance to daptomycin and host defense cationic antimicrobial peptides in clinical methicillin-resistant *Staphylococcus aureus* isolates. Antimicrob Agents Chemother **55:**4012–4018. http://dx.doi.org/10.1128/AAC.00223-11.
9. **Saravolatz LD, Pawlak J, Johnson L, Bonilla H, Saravolatz LD, II, Fakih MG, Fugelli A, Olsen WM.** 2012. *In vitro* activities of LTX-109, a synthetic antimicrobial peptide, against methicillin-resistant, vancomycin-intermediate, vancomycin-resistant, daptomycin-nonsusceptible, and linezolid-nonsusceptible *Staphylococcus aureus*. Antimicrob Agents Chemother **56:**4478–4482. http://dx.doi.org/10.1128/AAC.00194-12.
10. **Awasthi D, Kumar K, Ojima I.** 2011. Therapeutic potential of FtsZ inhibition: a patent perspective. Expert Opin Ther Pat **21:**657–679. http://dx.doi.org/10.1517/13543776.2011.568483.
11. **Lock RL, Harry EJ.** 2008. Cell-division inhibitors: new insights for future antibiotics. Nat Rev Drug Discov **7:**324–338. http://dx.doi.org/10.1038/nrd2510.
12. **Sass P, Brötz-Oesterhelt H.** 2013. Bacterial cell division as a target for new antibiotics. Curr Opin Microbiol **16:**522–530. http://dx.doi.org/10.1016/j.mib.2013.07.006.
13. **Schaffner-Barbero C, Martin-Fontecha M, Chacón P, Andreu JM.** 2012. Targeting the assembly of bacterial cell division protein FtsZ with small molecules. ACS Chem Biol **7:**269–277. http://dx.doi.org/10.1021/cb2003626.
14. **Vollmer W.** 2006. The prokaryotic cytoskeleton: a putative target for inhibitors and antibiotics? Appl Microbiol Biotechnol **73:**37–47. http://dx.doi.org/10.1007/s00253-006-0586-0.
15. **Adams DW, Errington J.** 2009. Bacterial cell division: assembly, maintenance and disassembly of the Z ring. Nat Rev Microbiol **7:**642–653. http://dx.doi.org/10.1038/nrmicro2198.
16. **Bi EF, Lutkenhaus J.** 1991. FtsZ ring structure associated with division in *Escherichia coli*. Nature **354:**161–164. http://dx.doi.org/10.1038/354161a0.
17. **Erickson HP, Anderson DE, Osawa M.** 2010. FtsZ in bacterial cytokinesis: cytoskeleton and force generator all in one. Microbiol Mol Biol Rev **74:**504–528. http://dx.doi.org/10.1128/MMBR.00021-10.
18. **Pinho MG, Errington J.** 2003. Dispersed mode of *Staphylococcus aureus* cell wall synthesis in the absence of the division machinery. Mol Microbiol **50:**871–881. http://dx.doi.org/10.1046/j.1365-2958.2003.03719.x.
19. **Pinho MG, MKjos Veening J-W.** 2013. How to get (a) round: mechanisms controlling growth and division of coccoid bacteria. Nat Rev Microbiol **11:**601–614. http://dx.doi.org/10.1038/nrmicro3088.
20. **Tan CM, Therien AG, Lu J, Lee SH, Caron A, Gill CJ, Lebeau-Jacob C, Benton-Perdomo L, Monteiro JM, Pereira PM, Elsen NL, Wu J, Deschamps K, Petcu M, Wong S, Daigneault E, Kramer S, Liang L, Maxwell E, Claveau D, Vaillancourt J, Skorey K, Tam J, Wang H, Meredith TC, Sillaots S, Wang-Jarantow L, Ramtohul Y, Langlois E, Landry F, Reid JC, Parthasarathy G, Sharma S, Baryshnikova A, Lumb KJ, Pinho MG, Soisson SM, Roemer T.** 2012. Restoring methicillin-resistant *Staphylococcus aureus* susceptibility to β-lactam antibiotics. Sci Transl Med **4:**126ra35. http://dx.doi.org/10.1126/scitranslmed.3003592.
21. **Andreu JM, Schaffner-Barbero C, Huecas S, Alonso D, Lopez-Rodriguez ML, Ruiz-Avila LB, Núñez-Ramírez R, Llorca O, Martín-Galiano AJ.** 2010. The antibacterial cell division inhibitor PC190723 is an FtsZ polymer-stabilizing agent that induces filament assembly and condensation. J Biol Chem **285:**14239–14246. http://dx.doi.org/10.1074/jbc.M109.094722.
22. **Elsen NL, Lu J, Parthasarathy G, Reid JC, Sharma S, Soisson SM, Lumb KJ.** 2012. Mechanism of action of the cell-division inhibitor PC190723: modulation of FtsZ assembly cooperativity. J Am Chem Soc **134:**12342–12345. http://dx.doi.org/10.1021/ja303564a.
23. **Haydon DJ, Stokes NR, Ure R, Galbraith G, Bennett JM, Brown DR, Baker PJ, Barynin VV, Rice DW, Sedelnikova SE, Heal JR, Sheridan JM, Aiwale ST, Chauhan PK, Srivastava A, Taneja A, Collins I, Errington J, Czaplewski LG.** 2008. An inhibitor of FtsZ with potent and selective anti-staphylococcal activity. Science **321:**1673–1675. http://dx.doi.org/10.1126/science.1159961.
24. **Stokes NR, Sievers J, Barker S, Bennett JM, Brown DR, Collins I, Errington VM, Foulger D, Hall M, Halsey R, Johnson H, Rose V, Thomaides HB, Haydon DJ, Czaplewski LG, Errington J.** 2005. Novel inhibitors of bacterial cytokinesis identified by a cell-based antibiotic screening assay. J Biol Chem **280:**39709–39715. http://dx.doi.org/10.1074/jbc.M506741200.
25. **Kaul M, Mark L, Zhang Y, Parhi AK, LaVoie EJ, Pilch DS.** 2013. Pharmacokinetics and *in Vivo* antistaphylococcal efficacy of TXY541, a 1-methylpiperidine-4-carboxamide prodrug of PC190723. Biochem Pharmacol **86:**1699–1707. http://dx.doi.org/10.1016/j.bcp.2013.10.010.
26. **Kaul M, Mark L, Zhang Y, Parhi AK, LaVoie EJ, Pilch DS.** 2013. An FtsZ-targeting prodrug with oral antistaphylococcal efficacy *in vivo*. Antimicrob Agents Chemother **57:**5860–5869. http://dx.doi.org/10.1128/AAC.01016-13.
27. **Sorto NA, Olmstead MM, Shaw JT.** 2010. Practical synthesis of PC190723, an inhibitor of the bacterial cell division protein FtsZ. J Org Chem **75:**7946–7949. http://dx.doi.org/10.1021/jo101720y.
28. **CLSI.** 2009. Methods for dilution antimicrobial susceptibility tests for bacteria that grow aerobically; approved standard, 8th ed, CLSI document M07-A8. Clinical and Laboratory Standards Institute, Wayne, PA.
29. **Balani SK, Zhu T, Yang TJ, Liu Z, He B, Lee FW.** 2002. Effective dosing regimen of 1-aminobenzotriazole for inhibition of antipyrine clearance in rats, dogs, and monkeys. Drug Metab Dispos **30:**1059–1062. http://dx.doi.org/10.1124/dmd.30.10.1059.
30. **Kaul M, Parhi AK, Zhang Y, LaVoie EJ, Tuske S, Arnold E, Kerrigan JE, Pilch DS.** 2012. A bactericidal guanidinomethyl biaryl that alters the dynamics of bacterial FtsZ polymerization. J Med Chem **55:**10160–10176. http://dx.doi.org/10.1021/jm3012728.
31. **Qi H, Lin C-P, Fu X, Wood LM, Liu AA, Tsai Y-C, Chen Y, Barbieri CM, Pilch DS, Liu LF.** 2006. G-quadruplexes induce apoptosis in tumor cells. Cancer Res **66:**11808–11816. http://dx.doi.org/10.1158/0008-5472.CAN-06-1225.
32. **Haydon DJ, Bennett JM, Brown D, Collins I, Galbraith G, Lancett P, Macdonald R, Stokes NR, Chauhan PK, Sutariya JK, Nayal N, Srivastava A, Beanland J, Hall R, Henstock V, Noula C, Rockley C, Czaplewski L.** 2010. Creating an antibacterial with *in vivo* efficacy: synthesis and characterization of potent inhibitors of the bacterial cell division protein FtsZ with improved pharmaceutical properties. J Med Chem **53:**3927–3936. http://dx.doi.org/10.1021/jm9016366.
33. **Adams DW, Wu LJ, Czaplewski LG, Errington J.** 2011. Multiple effects of benzamide antibiotics on FtsZ function. Mol Microbiol **80:**68–84. http://dx.doi.org/10.1111/j.1365-2958.2011.07559.x.
34. **Kaul M, Zhang Y, Parhi AK, LaVoie EJ, Tuske S, Arnold E, Kerrigan JE, Pilch DS.** 2013. Enterococcal and streptococcal resistance to PC190723 and related compounds: molecular insights from a FtsZ mutational analysis. Biochimie **95:**1880–1887. http://dx.doi.org/10.1016/j.biochi.2013.06.010.
35. **Gueiros-Filho FJ, Losick R.** 2002. A widely conserved bacterial cell division protein that promotes assembly of the tubulin-like protein FtsZ. Genes Dev **16:**2544–2556. http://dx.doi.org/10.1101/gad.1014102.

Supplementary Material

TXA709: A FtsZ-Targeting Benzamide Prodrug with Improved Pharmacokinetics and Enhanced *In Vivo* Efficacy against Methicillin-Resistant *Staphylococcus aureus*

Malvika Kaul, Lilly Mark, Yongzheng Zhang, Ajit K. Parhi, Yi Lisa Lyu, Joan Pawlak, Stephanie Saravolatz, Louis D. Saravolatz, Melvin P. Weinstein, Edmond J. LaVoie, and Daniel S. Pilch#

#Address correspondence to Daniel S. Pilch, pilchds@rwjms.rutgers.edu

SUPPLEMENTAL EXPERIMENTAL METHODS

Synthesis of TXA707 and TXA709. The synthesis of TXA707 (compound **5**) and TXA709 (compound **7**) is outlined in Scheme 1 below. The chloromethyl intermediate **3** was prepared from commercially available 2-chloro-5-(trifluoromethyl)pyridin-3-amine in two steps. The acylation of **1** with commercially available chloroacetyl chloride afforded 2-chloro-N-(2-chloro-5-(trifluoromethyl)pyridine-3-yl)acetamide **2**, which was then subjected to sulfurization followed by ring closure using previously published conditions (1) to produce intermediate chloro compound **3** in good overall yield. Coupling of **3** with the known phenol **4** (2) using $NaHCO_3$ provided TXA707 (compound **5**) in 61% yield. The treatment of commercially available 1-methylpiperidine-4-carboxylic acid hydrochloride with $SOCl_2$ afforded the acid chloride **6**, which was then reacted with TXA707 (compound **5**) using NaH in the presence of a catalytic amount of water to generate TXA709 (compound **7**) in 44% yield. All stock solutions of TXA707 and TXA709 were prepared in DMSO, and stored at -20 °C prior to their use in any experiment.

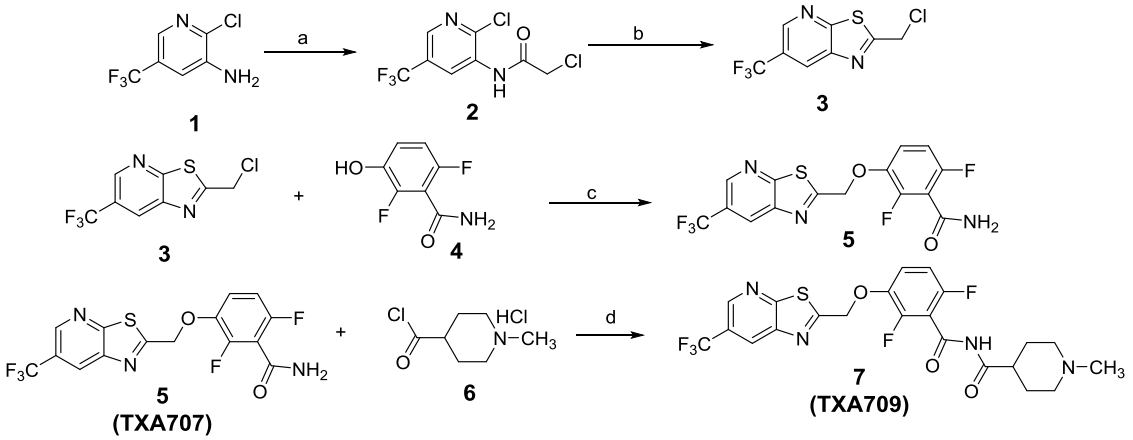

Scheme 1 reagents and conditions: (a) Chloroacetyl chloride, Et_3N, DCM, 2 hours, 83%; (b) P_5S_{10}, toluene, 115 °C, 30 minutes, 74%; (c) $NaHCO_3$, DMF, 50 °C, 12 hours, 61%; (d) NaH, cat. H_2O, 10 minutes, 44%.

General chemistry methods. Column chromatography refers to flash chromatography conducted on disposable normal phase Teledyne ISCO silica columns with a CombiFlash Rf Teledyne ISCO using the solvent systems indicated. Proton and carbon nuclear magnetic resonance (^{1}H and ^{13}C NMR, respectively) were recorded using either a Bruker 400 MHz or a Varian 300 MHz Unity Inova spectrometer in the deuterated solvent indicated, with chemical shifts reported in δ units downfield from tetramethylsilane (TMS). Coupling constants are reported in hertz (Hz). 2-Chloro-5-(trifluoromethyl)pyridin-3-amine and 1-methylpiperidine-4-carboxylic acid hydrochloride were obtained from Combi-Blocks, LLC. All other starting materials and reagents were obtained from Aldrich. Solvents were purchased from Fisher Scientific, and were A.C.S. or HPLC grade. Methylene chloride was freshly distilled from calcium hydride. All other solvents were used as provided without further purification.

2-Chloro-N-(2-chloro-5-(trifluoromethyl)pyridin-3-yl)acetamide (compound **2**) was synthesized as follows: A 100-mL round bottom flask equipped with a magnetic stirrer was charged with 2-chloro-5-(trifluoromethyl)pyridin-3-amine (5.0 g , 25.4 mmol), CH_2Cl_2 (100 mL), and TEA (7.08 mL, 50.8 mmol). The reaction mixture was cooled under an ice-bath and chloroacetyl chloride (4.04 mL, 50.8 mmol) was slowly added. The reaction mixture was stirred at room temperature for 2 hours. The reaction mixture was then diluted with CH_2Cl_2 (100 mL), washed with 1 N HCl, saturated $NaHCO_3$, and brine. The CH_2Cl_2 solution was dried over Na_2SO4, and concentrated to give a residue, which was purified by column chromatography using 20% EtOAc/hexane to afford compound **2** as an off white solid (5.8 g, 83%). ^{1}H NMR (300 MHz, $CDCl_3$) δ: 9.05 (s, 2H), 8.44 (s, 1H), 4.27 (s, 2H).

2-(Chloromethyl)-6-(trifluoromethyl)thiazolo[5,4-b]pyridine (compound **3**) was synthesized as follows: A 100-mL round bottom flask equipped with a magnetic stirrer was

charged with 2-chloro-N-(2-chloro-5-(trifluoromethyl)pyridin-3-yl)acetamide (5.8 g, 21.2 mmol), P_5S_{10} (3.6 g), and toluene (100 mL). The resulting mixture was refluxed at 115 °C for 30 minutes. The reaction mixture was cooled to room temperature and the solids were filtered off. The solvent was removed and the crude product was purified by column chromatography using 5% EtOAc/hexane to afford the product as a light yellow solid (4.0 g, 74% yield). ^{1}H NMR (300 MHz, $CDCl_3$) δ: 8.90 (s, 1H), 8.50 (s, 1H), 4.98 (s, 2H). ^{13}C NMR (100 MHz, DMSO-d_6) δ 170.6, 161.7, 144.4, 144.1, 128.0, 124.5, 124.3, 123.9, 123.6, 123.3, 122.2, 119.5, 42.1.

TXA707 (compound **5**) was synthesized as follows: A 25-mL round bottom flask equipped with a magnetic stirrer was charged with compound **3** (3.74 g, 14.8 mmol), DMF (30 mL), $NaHCO_3$ (2.37 g, 28.2 mmol), and compound **4** (2.44 g, 14.1 mmol). The reaction mixture was heated at 50 °C overnight. After cooling to room temperature, water was added to the reaction mixture, and the precipitate was collected by filtration to give a brown solid. After drying, the crude product was triturated with CH_2Cl_2 to afford the desired product as a light brown solid. The brown solid was recrystallized with EtOAc to afford a crystalline light purple solid (3.5 g, 61% yield). ^{1}H NMR (300 MHz, DMSO-d_6) δ: 9.05 (s, 1H), 8.93 (s, 1H), 8.17 (bs, 1H), 7.89 (bs, 1H), 7.45-7.37 (m, 1H), 7.11 (m, 1H), 5.77 (s, 2H). ^{13}C NMR (100 MHz, DMSO-d_6) δ 171.3, 161.2, 161.0, 153.9, 151.5, 146.9, 144.5, 143.8, 141.8, 127.9, 127.8, 125.0, 123.8, 123.5, 122.8, 116.9, 116.5, 111.1, 69.0. HRMS calculated for $C_{15}H_8F_5N_3O_2S$ $(M + H)^+$, 390.0317; found, 390.0330.

TXA709 (compound **7**) was synthesized as follows: A 100-mL round bottom flask equipped with a magnetic stirrer was charged with TXA707 (compound **5**) (1.0 g, 2.57 mmol), compound **6** (1.0 g, 5.05 mmol), and THF (20 mL). With stirring, NaH (600 mg, 15 mmol, 60% dispersion in mineral oil) was added portion-wise over five minutes. The resulting reaction

mixture was stirred for 10 minutes. A solution of water (40 µL) in THF (2 mL) was then added via a pipet over five minutes. The reaction mixture changed from a suspension to a brown solution. After completion, the reaction was quenched by the addition of a few drops of water, and then diluted with dichloromethane. The organic phase was separated, washed with brine, and dried over Na_2SO_4. The solvent was removed under reduced pressure, and the resulting residue purified by ISCO chromatography using 10 % MeOH in DCM + 1% NH_4OH to afford a light brown solid, which was then triturated with EtOAc to give a beige solid (590 mg, 44% yield). ^{1}H NMR (300 MHz, $CDCl_3$) δ: 8.58 (s, 1H), 8.31 (broad s, 1H), 8.24 (s, 1H), 7.24-7.14 (m, 1H), 6.94-6.87 (m, 1H), 5.50 (s, 2H), 2.94-2.80 (m, 3H), 2.28 (s, 3H), 2.10-1.74 (m, 6H). ^{13}C NMR (100 MHz, DMSO-d_6) δ 174.9, 171.1, 161.2, 160.3, 153.5, 151.1, 149.1, 146.6, 144.5, 143.8, 141.8, 141.7, 127.8, 125.0, 124.1, 123.8, 123.5, 123.2, 122.3, 129.6, 117.6, 117.5, 115.9, 117.7, 115.6, 111.4, 111.1, 69.1, 54.8, 54.4, 45.9, 41.9, 27.6. HRMS calculated for $C_{22}H_{19}F_5N_4O_3S$ $(M + H)^+$, 515.1171; found, 515.1181.

***In vivo* efficacy studies – murine peritonitis model.** All studies were conducted in full compliance with the standards established by the US National Research Council's Guide for the Care and Use of Laboratory Animals, and were approved by the Institutional Animal Care and Use Committee (IACUC) of Rutgers University. Groups of four to six female Swiss-Webster mice with an average weight of 25 g were infected intraperitoneally with a lethal inoculum of a given bacterial strain in saline. The inocula of MRSA ATCC 43300, MRSA Mu3, and MSSA ATCC 19636 contained 1.25 x 10^8, 5 x 10^7, and 5 x 10^6 CFUs of bacteria, respectively. The inocula also contained porcine mucin (Sigma) at a (wt/vol) percentage of 5% (in the ATCC 43300 and Mu3 inocula) or 1.5% (in the ATCC 19636 inoculum). The composition of the lethal inoculum for each bacterial strain was determined by titration of both bacterial CFU and mucin

percentage. The inocula were prepared by combining overnight cultures with sterile 10% mucin to achieve the desired bacterial CFU and mucin percentage. The bacterial load in each inoculum was verified by plating serial dilutions. The mice were fasted overnight prior to their use in oral studies.

The body temperatures of all mice were monitored for a period of five days after infection. Body temperatures were recorded at the Xiphoid process using a noninvasive infrared thermometer (Braintree Scientific, Inc.). Infected mice with body temperatures ≤28.9 °C were viewed as being unable to recover from the infection (3) and were euthanized.

Studies with TXY541 and ABT. Two sets of oral (p.o.) experiments probed the impact of ABT on the efficacy of TXY541 versus MSSA ATCC 19636 and MRSA ATCC 43300. The vehicle for TXY541 was 10 mM citrate (pH 2.6), and the vehicle for ABT was water. Four groups of six infected mice were used in the MSSA 19636 experiments. Groups 1 and 2 were pretreated with a 50 mg/kg dose of ABT one hour prior to infection, while Groups 3 and 4 did not receive pretreatment. Following infection, the mice in Group 1 were treated with citrate vehicle, the mice in Groups 2 and 3 were treated with 64 mg/kg TXY541 (in two divided doses of 32 mg/kg), and the mice in Group 4 were treated with 128 mg/kg TXY541 (in four divided doses of 32 mg/kg). The first dose of TXY541 was administered 10 minutes after infection, with subsequent doses being administered at 12-minute intervals thereafter. In the MRSA ATCC 43300 experiments, four groups of six mice were also used. Groups 1 and 2 were pretreated with a 50 mg/kg dose of ABT one hour prior to infection, while Groups 3 and 4 did not receive pretreatment. Following infection, the mice in Group 1 were treated with citrate vehicle, the mice in Groups 2 and 3 were treated with 64 mg/kg TXY541 (in two divided doses of 32 mg/kg), and the mice in Group 4 were treated with 192 mg/kg TXY541 (in six divided doses of 32

mg/kg). The first dose of TXY541 was administered 60 minutes after infection, with subsequent doses being administered at 12-minute intervals thereafter. The dosing volume for TXY541 and ABT was 16 and 8 mL/kg, respectively.

Oral (p.o.) studies with TXA709. In the studies with MSSA ATCC 19636, four experimental groups of six infected mice were treated as follows: Group 1 – untreated; Group 2 –vehicle only; Group 3 – 32 mg/kg TXA709; and Group 4 – 64 mg/kg TXA709 (in two divided doses of 32 mg/kg). In the studies with MRSA ATCC 43300 and Mu3, four groups of infected mice were treated as follows: Group 1 – untreated; Group 2 –vehicle only; Group 3 – 48 mg/kg TXA709 (in two divided doses of 24 mg/kg); and Group 4 – 96 mg/kg TXA709 (in four divided doses of 24 mg/kg). Each experimental group contained four mice in the MRSA ATCC 43300 studies and six mice in the MRSA Mu3 studies. In both the MSSA 19636 and MRSA Mu3 studies, the first dose of TXA709 was administered 10 minutes after infection, with subsequent doses being administered at 12-minute intervals thereafter. In the MRSA 43300 studies, the first dose of TXA709 was administered 60 minutes after infection, with subsequent doses being administered at 12-minute intervals thereafter.. In all studies, the vehicle for TXA709 was 10 mM citrate (pH 2.6), and the dosing volume was 16 mL/kg.

Intravenous (i.v.) studies with TXA709. In the studies with MSSA ATCC 19636 and MRSA ATCC 43300, four experimental groups of infected mice were treated as follows: Group 1 – untreated; Group 2 – citrate vehicle only; Group 3 – 36 mg/kg TXA709; and Group 4 – 72 mg/kg TXA709 (in two divided doses of 36 mg/kg). Each experimental group contained five mice in the MSSA ATCC 19636 studies and six mice in the MRSA ATCC 43300 studies. In the MRSA Mu3 studies, five groups of six infected mice were treated as follows: Group 1 – untreated; Group 2 – citrate vehicle only; Group 3 – 24 mg/kg TXA709; Group 4 – 48 mg/kg

TXA709 (in two divided doses of 24 mg/kg); and Group 5 – 72 mg/kg TXA709 (in three divided doses of 24 mg/kg). The dosing intervals were as described above for the p.o. studies, and the dosing volume was 12 mL/kg.

***In vivo* efficacy studies – murine thigh model.** These studies were conducted by Eurofins Panlabs, Inc. (Taipei, Taiwan). Groups of five male ICR (CD-1) mice weighing 22 ± 2 g were used. The mice were immunosuppressed by two intraperitoneal injections of 100 mg/kg cyclophosphamide at four and two days prior to infection. Animals were inoculated intramuscularly (0.1 mL/thigh) with 10^5 CFU/mouse of MRSA ATCC 33591 in the right thigh. TXA709 was formulated in 10 mM citrate vehicle, and was administered p.o. at 120 mg/kg (40 mg/kg x 3 at 2, 3, and 4 hours post-infection) to one test group of mice and at 160 mg/kg (40 mg/kg x 4 at 2, 3, 4, and 5 hours post-infection) to a second test group. The dosing volume of TXA709 in both test groups was 20 mL/kg. A negative control group received citrate vehicle p.o. at 2, 3, 4, and 5 hours post-infection. A positive control group of mice received vancomycin i.v. at 60 mg/kg (30 mg/kg x 2 at 2 and 8 hours post-infection). At 24 hours post-infection, the mice were euthanized, and the right thigh muscle was harvested from each animal. The muscle tissues were homogenized, and the homogenates were plated on nutrient agar plates for CFU determination.

SUPPLEMENTAL REFERENCES

1. **Ding, Z.-C., W. Zhou and X. Ma.** 2012. A Facile Approach to the Synthesis of 3-(6-Chloro-thiazolo[5,4-b]pyridin-2-ylmethoxy)-2,6-difluoro-benzamide (PC190723). Synlett **23:**1039-1042.
2. **Haydon, D. J., J. M. Bennett, D. Brown, I. Collins, G. Galbraith, P. Lancett, R. Macdonald, N. R. Stokes, P. K. Chauhan, J. K. Sutariya, N. Nayal, A. Srivastava, J. Beanland, R. Hall, V. Henstock, C. Noula, C. Rockley and L. Czaplewski.** 2010. Creating an Antibacterial with *in Vivo* Efficacy: Synthesis and Characterization of Potent

Inhibitors of the Bacterial Cell Division Protein FtsZ with Improved Pharmaceutical Properties. J. Med. Chem. **53:**3927-3936.

3. **Stiles, B. G., Y. G. Campbell, R. M. Castle and S. A. Grove.** 1999. Correlation of Temperature and Toxicity in Murine Studies of Staphylococcal Enterotoxins and Toxic Shock Syndrome Toxin 1. Infect. Immun. **67:**1521-1525.

SUPPLEMENTAL FIGURE

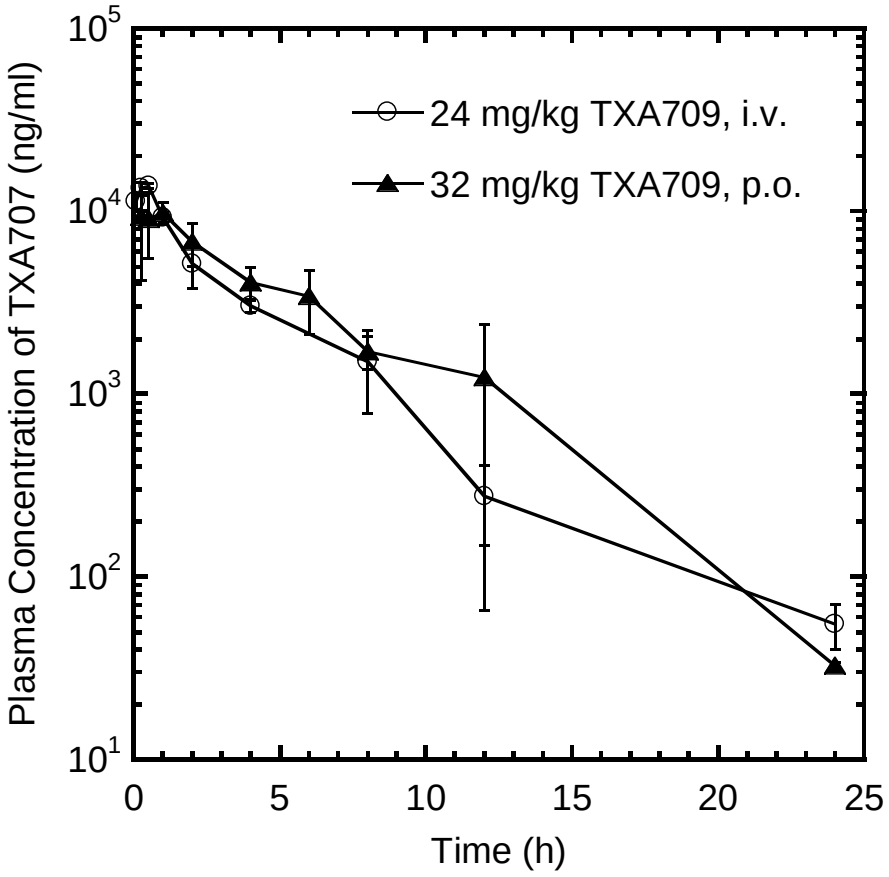

FIG S1 Time-dependent plasma concentrations of TXA707 following either a single intravenous (i.v.) dose of 24 mg/kg TXA709 (open circles) or a single oral (p.o.) dose of 32 mg/kg TXA709 (filled circles) to male BALB/c mice.